Available online at www.sciencedirect.com

SciVerse ScienceDirect

Journal of the Franklin Institute 349 (2012) 1087–1105

Journal of The Franklin Institute

www.elsevier.com/locate/jfranklin

Adaptive backstepping trajectory tracking control of robot manipulator

Qinglei Hu*, Liang Xu, Aihua Zhang

Department of Control Science and Engineering, Harbin Institute of Technology, Harbin 150001, China

Received 1 June 2011; received in revised form 29 August 2011; accepted 2 January 2012
Available online 12 January 2012

Abstract

An adaptive backstepping control scheme is proposed for task-space trajectory tracking of robot manipulators in the presence of uncertain parameters and external disturbances. In the case of external disturbance-free, the developed controller guarantees that the desired trajectory is globally asymptotically followed. Moreover, taking disturbances into consideration, the controller is synthesized by using adaptive technique to estimate the system uncertainties. It is shown that L_2 gain of the closed-loop system is allowed to be chosen arbitrarily small so as to achieve any level of L_2 disturbance attenuation. The associated stability proof is constructive and accomplished by the development of a Lyapunov function candidate. Numerical simulation results are included to verify the control performance of the control approach derived.

1. Introduction

The design of robust control system for robot manipulators in the presence of model uncertainties is one of the most challenging tasks for control engineers. In the past decades, several control algorithms are proposed to fulfill this objective (for example, Refs. [1–5]). The design of those controllers relies on the assumption that the exact kinematics (i.e. Jacobian matrix) of robot manipulators is known. Unfortunately, in practical, no physical parameters can be measured precisely in advance. And, when the robot picks up objects of different lengths or unknown orientations, the overall kinematics are changing and therefore, difficult to derive exactly. Besides, in some special robot systems such as space

*Corresponding author.
E-mail addresses: huqinglei@hit.edu.cn, qlhu@ntu.edu.sg (Q. Hu).

doi:10.1016/j.jfranklin.2012.01.001

manipulator systems, the Jacobian matrix not only contains kinematic terms but also involves dynamic parameters. All these conditions suggest that the kinematic uncertainty must be taken into consideration when designing controllers.

To overcome the problem of uncertain kinematics, several approximate Jacobian setpoint controllers [6–8] are proposed. In Ref. [6] a feedback control law for robots with uncertain kinematics and dynamics is designed to drive the ender-effector to the desired position. The experimental tests are also conducted later and the results are shown in Ref. [7]. In Ref. [8], considering the kinematic and dynamic uncertainties, an amplitude-limited torque input controller is designed to achieve the semi-global asymptotic stabilization of the task-space setpoint control error.

However, these researches are focused on setpoint control of robots. While in most applications, it is necessary to specify the motion in much more details than just simply stating the desired final position. Thus, considering the trajectory tracking control problem would be much more meaningful. Recently, an adaptive Jacobian controller was proposed to achieve the trajectory tracking control objects of robot manipulators [9–13]. In Ref. [9], a new approximate Jacobian adaptive controller is proposed for trajectory tracking of robots with uncertain kinematics and dynamics and experiments are conducted to illustrate the performance of this controller. In Ref. [10] an actuator model is taken into consideration when designing the trajectory tracking controller. In Ref. [11] only the information of end-effector position in visual space and the robot's joint angles and velocities are needed in the synthesis of the controller. In Ref. [12], the controller is designed without requiring the information of the task-space and joint-space velocity. Theoretically, all the mentioned methods can achieve task-space trajectory tracking control objects under both kinematic and dynamic uncertainties. But, few of those papers make any further discussions on the explicit role each designed parameter performs in the closed-loop behaviors, which is critically important for the real application of those controllers.

Backstepping technique provides a systematic closed loop construction means of Lyapunov function to a broad class of strict-feedback nonlinear systems. Due to its simple cofiguration and ease of implementation, this control strategy is widely applied to the various control systems, such as output feedback control of nonlinear systems [14,15], control of electrohydraulic servos systems [16], spacecraft slew maneuver problems [17] and so on. Recently, in some research literatures, a novel method to analyze the explicit functions of the designed parameters in backstepping controllers is developed [18–20]. In Ref. [19], an observer-based backstepping output control scheme is proposed for stabilizing and controlling a class of uncertain chaotic systems. Not only the global stability is guaranteed by the proposed controller, but also the transient and asymptotic tracking performances are quantified as explicit functions of the design parameters. In Ref. [20], a robust adaptive controller is proposed for uncertain systems with unknown input time-delay to achieve the asymptotic stable. And the tracking performance is also qualified as explicit functions of design parameters. With this technique, transient performance can be established and improved with explicit tuning of design parameters which helps a lot in obtaining the desired closed-loop behaviors.

In this work, an adaptive backstepping control scheme is developed to achieve the task space trajectory tracking control objects for robot manipulators in the presence of kinematic/dynamic uncertainty and external disturbances. Theoretical stabilization is proved and the detailed functions of tuning parameters in the proposed controller are discussed. Moreover, taking disturbance torque into consideration, the L_2 gain performance analysis is achieved to evaluate the tracking performance. It is shown that the L_2 gain from disturbance torque to controlled output can meet the required demand by means of appropriately choosing controller gains. In addition, this method does not need to measure the joint acceleration which to some extent ensures the robustness of the proposed controller. The paper is organized as follows: in the following section, we provide a formal problem statement accompanied by all the governing equations. In Section 3, we propose control scheme and provide the associated stability analysis for the resulting closed-loop dynamics. Section 4 presents numerical simulation results, and the paper is closed with some concluding remarks.

Notions: Through out the paper, let $\mathbb{R}$ be the real number and $\mathbb{R}^n$ denote the space of real n-dimensional vector. The norm of a vector $\boldsymbol{x} \in \mathbb{R}^n$ is defined as $\|\boldsymbol{x}\| = \sqrt{\boldsymbol{x}^{\mathrm{T}}\boldsymbol{x}}$. The $\mathscr{L}_2$-norm of piecewise continuous, square-integrable function $\boldsymbol{u} : [0,\infty) \to \mathbb{R}^n$ is defined as $\|\boldsymbol{u}\|_{\mathscr{L}_2} = \int_0^\infty \boldsymbol{u}(t)^{\mathrm{T}}\boldsymbol{u}(t)\,\mathrm{d}t$.

2. Mathematical model of robot manipulator

The dynamic model for a rigid n-link, serially connected, direct driven revolute robot is given in joint space as follows [21]:

$$\boldsymbol{M}(\boldsymbol{q})\ddot{\boldsymbol{q}}+\boldsymbol{C}(\boldsymbol{q},\dot{\boldsymbol{q}})\dot{\boldsymbol{q}}+\boldsymbol{g}(\boldsymbol{q}) = \boldsymbol{\tau} + \boldsymbol{\tau}_d \tag{1}$$

where $\boldsymbol{q},\dot{\boldsymbol{q}},\ddot{\boldsymbol{q}} \in \mathbb{R}^n$ denote joint angle, velocity and acceleration vectors, respectively; $\boldsymbol{M}(\boldsymbol{q}) \in \mathbb{R}^{n\times n}$ represents the robot inertial matrix; $\boldsymbol{C}(\boldsymbol{q},\dot{\boldsymbol{q}})\dot{\boldsymbol{q}},\boldsymbol{g}(\boldsymbol{q})$ and $\boldsymbol{\tau} \in \mathbb{R}^n$ denote the centripetal-coriolis force, the gravitational force and control inputs, respectively; $\boldsymbol{\tau}_d \in \mathbb{R}^n$ is the external disturbance which satisfies $\|\boldsymbol{\tau}_d\| \le \delta_d$ where δ_d is a known positive constant.

Note that the dynamic model introduced in Eq. (1) has the following properties which are helpful in subsequent control development and analysis [22]:

Property 1. *The positive-definite and symmetric inertia matrix, satisfies the following inequalities*:

$$m_1\|\zeta\|^2 \le \zeta^{\mathrm{T}}\boldsymbol{M}(\boldsymbol{q})\zeta \le m_2\|\zeta\|^2 \quad \forall \zeta \in \mathbb{R}^n \tag{2}$$

where $m_1,m_2 \in \mathbb{R}$ are known positive bounding constants.

Property 2. *The time derivative of the inertia matrix and the centripetal-Coriolis matrix satisfy the following skew symmetric relationship*:

$$\zeta^{\mathrm{T}}(\dot{\boldsymbol{M}}(\boldsymbol{q})-2\boldsymbol{C}(\boldsymbol{q},\dot{\boldsymbol{q}}))\zeta = 0 \quad \forall \zeta \in \mathbb{R}^n \tag{3}$$

Property 3. *The dynamic model is linear with respect to a set of physical parameters $\boldsymbol{\theta}_d = [\theta_{d1},\theta_{d2},\ldots,\theta_{dp}]^{\mathrm{T}}$*

$$\boldsymbol{M}(\boldsymbol{q})\ddot{\boldsymbol{q}}+\boldsymbol{C}(\boldsymbol{q},\dot{\boldsymbol{q}})\dot{\boldsymbol{q}}+\boldsymbol{g}(\boldsymbol{q}) = \boldsymbol{Y}_d(\boldsymbol{q},\dot{\boldsymbol{q}},\dot{\boldsymbol{q}},\ddot{\boldsymbol{q}})\boldsymbol{\theta}_d \tag{4}$$

where $\boldsymbol{Y}_d(\bullet) \in \mathbb{R}^{n\times p}$ is called dynamic regressor matrix.

Let $\boldsymbol{x} \in \mathbb{R}^m (m \le n)$ represents a task space vector that is related to the robot joint-space as

$$\boldsymbol{x} = \boldsymbol{h}(\boldsymbol{q}), \quad \dot{\boldsymbol{x}} = J\dot{\boldsymbol{q}} \tag{5}$$

where $\boldsymbol{h}(\boldsymbol{q}) \in \mathbb{R}^m$ denotes the differentiable forward kinematics of the manipulator, and $\boldsymbol{J}(\boldsymbol{q}) \triangleq (\partial\boldsymbol{h}/\partial\boldsymbol{q}) \in \mathbb{R}^{m\times n}$ represents the differentiable manipulator Jacobian matrix.

Property 4. *$\boldsymbol{J}(\boldsymbol{q})\dot{\boldsymbol{q}}$ is linear in a set of constant parameters $\boldsymbol{\theta}_k = [\theta_{k1},\theta_{k2},\ldots,\theta_{kq}]^{\mathrm{T}}$ contained in the Jacobian matrix*

$$\boldsymbol{J}(\boldsymbol{q})\dot{\boldsymbol{q}} = \boldsymbol{Y}_k(\boldsymbol{q},\dot{\boldsymbol{q}})\boldsymbol{\theta}_k \tag{6}$$

where $\boldsymbol{Y}_k(\,\bullet) \in \mathbb{R}^{m\times q}$ is called the kinematic regressor matrix. In the following sections, we refer these parameters $\boldsymbol{\theta}_k$ as "kinematic parameters" even though they may actually contain dynamic terms such as link mass in specific robot manipulator systems.

The subsequent development is also based on the assumption that all kinematic singularities associated with $\boldsymbol{J}(\boldsymbol{q})$ are assumed always to be avoided. For the control synthesis, the exact kinematic and dynamic parameters are assumed not to be known. The estimations $\hat{\boldsymbol{\theta}}_k,\hat{\boldsymbol{\theta}}_d$ are adopted to make an approximation of actual physical parameters. The control objectives are to design adaptive backstepping control law $\boldsymbol{\tau}$ such that

- The tracking error $\boldsymbol{x}-\boldsymbol{x}_d$ is globally asymptotically stable when the disturbance torque $\boldsymbol{\tau}_d$ is assumed to be zero.
- When taking the disturbance torque $\boldsymbol{\tau}_d$ into consideration, the L_2 gain of the closed loop system is less than the given value γ.

The synthesis of the controller is also based on the assumptions that $\boldsymbol{x},\boldsymbol{q},\dot{\boldsymbol{q}}$ are measurable. Specifically, $\boldsymbol{q}$ and $\dot{\boldsymbol{q}}$ can be obtained from encoder/tachometer sensors, and $\boldsymbol{x}$ could be obtained from a camera system.

3. Adaptive backstepping controller design

Backstepping is a recursive Lyapunov-based scheme. The idea of adaptive backstepping is to design a controller recursively by considering some of the state variables as "virtual controls" and designing them for intermediate control laws. To give a velar ideal of such development, the following change of coordinate is made:

$$z_1 = \boldsymbol{x}-\boldsymbol{x}_d \tag{7}$$

$$z_2 = \dot{\boldsymbol{q}}-\phi \tag{8}$$

where ϕ is the virtual control for system in Eq. (7) to be determined. Careful examination reveals that z_1 actually is the trajectory tracking error. And ϕ can be regarded as a reference joint velocity. Consequently, z_2 is the joint velocity tracking error. To this end, the proposed control algorithm can be made up of two closed-up controllers: the task-space trajectory tracking one and the joint-space velocity tracking one. The control diagram of the whole system is illustrated in Fig. 1.

Note that the trajectory tracking controller is designed for the kinematic subsystem in Eq. (7), and by assuming the joint velocity as virtual control input and taking the tracking error as systemic output, the trajectory tracking controller generates a reference velocity ϕ and a kinematic parameter update law which is designed to deal with the kinematic parameter uncertainty. Then backstepping the reference joint velocity into the dynamic subsystem in Eq. (8), the additional control torque and dynamic parameter update law are derived to achieve the task space trajectory tracking control of robot manipulator system.

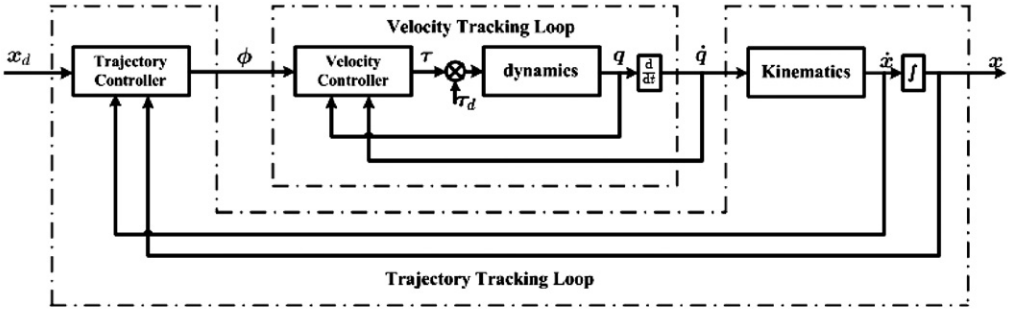

Fig. 1. Control diagram of the whole system.

Step 1: Let the controlled output is defined as

$$y = [\,\rho_1 z_1 \quad \rho_2 \boldsymbol{s} \quad \rho_3 z_2\,]^{\mathrm{T}} \tag{9}$$

where the auxiliary sliding vector $\boldsymbol{s}$ has the form of

$$\boldsymbol{s} \triangleq \dot{\boldsymbol{z}}_1 + \alpha \boldsymbol{z}_1 \tag{10}$$

where α is a positive constant.

Furthermore, the approximate estimation of $\boldsymbol{s}$ can be constructed using joint velocity as

$$\hat{\boldsymbol{s}} = \hat{\boldsymbol{J}}\dot{\boldsymbol{q}} - \dot{\boldsymbol{x}}_d + \alpha \boldsymbol{z}_1 \tag{11}$$

To this end, the estimation error of $\boldsymbol{s}$ is calculated to be

$$\boldsymbol{s} - \hat{\boldsymbol{s}} = \boldsymbol{Y}_k \tilde{\boldsymbol{\theta}}_k \tag{12}$$

where $\tilde{\boldsymbol{\theta}}_k \triangleq \boldsymbol{\theta}_k - \hat{\boldsymbol{\theta}}_k$.

In the following sections, the adaptive backstepping control scheme is proposed to accomplish the task space tracking control objective. From robotic kinematics in Eq. (5), the dynamic equation of the trajectory tracking error can be obtained as

$$\dot{\boldsymbol{z}}_1 = \hat{\boldsymbol{J}}\dot{\boldsymbol{q}} + \boldsymbol{Y}_k \tilde{\boldsymbol{\theta}}_k - \dot{\boldsymbol{x}}_d \tag{13}$$

It can be seen that Eq. (13) can be regarded as kinematic subsystem of the robot manipulator related to the trajectory tracking error where defining joint velocity $\dot{\boldsymbol{q}}$ as control input and tracking error z_1 as output. Here, we first design the virtual control ϕ for the kinematic subsystem.

Choosing Lyapunov function as

$$V_1 = \tfrac{1}{2}\boldsymbol{z}_1{}^{\mathrm{T}}\boldsymbol{z}_1 + \tfrac{1}{2}\tilde{\boldsymbol{\theta}}_k{}^{\mathrm{T}}\boldsymbol{\Gamma}_k^{-1}\tilde{\boldsymbol{\theta}}_k + \boldsymbol{\theta}_k^{\mathrm{T}}\mathrm{diag}[\boldsymbol{\mu}(\mathrm{t})]\boldsymbol{\theta}_k \tag{14}$$

where $\boldsymbol{\Gamma}_k \triangleq \mathrm{diag}[\kappa_{k1}, \kappa_{k2}, \ldots, \kappa_{kq}]$ is a positive definite diagonal matrix, and the vector function $\mu(t)$ is defined as $\boldsymbol{\mu}(t) \triangleq [\mu_1(t), \mu_2(t), \ldots, \mu_q(t)]^{\mathrm{T}}$ with initial values set to be positive.

Then the derivative of V_1 along with Eq.(13) is given as

$$\begin{aligned} \dot{V}_1 &= \boldsymbol{z}_1^{\mathrm{T}}\dot{\boldsymbol{z}}_1 + \tilde{\boldsymbol{\theta}}_k{}^{\mathrm{T}}\boldsymbol{\Gamma}_k^{-1}\dot{\tilde{\boldsymbol{\theta}}}_{\mathbf{k}} + \boldsymbol{\theta}_k^{\mathrm{T}}\mathrm{diag}[\dot{\boldsymbol{\mu}}(t)]\boldsymbol{\theta}_k \\ &= \boldsymbol{z}_1^{\mathrm{T}}(\hat{\boldsymbol{J}}\dot{\boldsymbol{q}} + \boldsymbol{Y}_k\tilde{\boldsymbol{\theta}}_k - \dot{\boldsymbol{x}}_d) + \tilde{\boldsymbol{\theta}}_k^{\mathrm{T}}\boldsymbol{\Gamma}_k^{-1}\dot{\tilde{\boldsymbol{\theta}}}_{\mathbf{k}} + \boldsymbol{\theta}_k^{\mathrm{T}}\mathrm{diag}[\dot{\boldsymbol{\mu}}(\boldsymbol{t})]\boldsymbol{\theta}_k \\ &= \boldsymbol{z}_1^{\mathrm{T}}(\hat{\boldsymbol{J}}\boldsymbol{z}_2 + \hat{\boldsymbol{J}}\boldsymbol{\phi} - \dot{\boldsymbol{x}}_d) - \tilde{\boldsymbol{\theta}}_k^{\mathrm{T}}(\boldsymbol{\Gamma}_k^{-1}\dot{\hat{\boldsymbol{\theta}}}_k - \boldsymbol{Y}_k^T\boldsymbol{z}_1) + \boldsymbol{\theta}_k^{\mathrm{T}}\mathrm{diag}[\dot{\boldsymbol{\mu}}(\boldsymbol{t})]\boldsymbol{\theta}_k \end{aligned} \tag{15}$$

In order to arrange the foregoing equation to be negative definite, the virtual control ϕ and kinematic parameter update law are chosen

$$\phi = \hat{\boldsymbol{J}}^{-}1(-\alpha \boldsymbol{z}_1 + \dot{\boldsymbol{x}}_d) \tag{16}$$

$$\dot{\hat{\boldsymbol{\theta}}}_k = \boldsymbol{\Gamma}_k(\boldsymbol{Y}_k{}^{\mathrm{T}}\boldsymbol{z}_1 + 2\beta \boldsymbol{Y}_k{}^{\mathrm{T}}\boldsymbol{s}) - \mathrm{diag}[\boldsymbol{\mu}(t)]\hat{\boldsymbol{\theta}}_k,\ \dot{\boldsymbol{\mu}}(\mathrm{t}) = -\boldsymbol{\Gamma}_k{}^{-1}\boldsymbol{\mu}(t) \tag{17}$$

where β is a positive constant.

Then, substituting Eqs. (16) and (17) into Eq. (15) yields

$$\dot{V}_1 = -\alpha \boldsymbol{z}_1^{\mathrm{T}}\boldsymbol{z}_1 + \boldsymbol{z}_1^{\mathrm{T}}\hat{\boldsymbol{J}}\boldsymbol{z}_2 - 2\beta\tilde{\boldsymbol{\theta}}_k^{\mathrm{T}}\boldsymbol{Y}_k^{\mathrm{T}}\boldsymbol{s} + (\tilde{\boldsymbol{\theta}}_k^{\mathrm{T}}\boldsymbol{\Gamma}_k^{-1}\mathrm{diag}[\boldsymbol{\mu}(t)]\hat{\boldsymbol{\theta}}_k - \boldsymbol{\theta}_k^{\mathrm{T}}\boldsymbol{\Gamma}_k^{-1}\mathrm{diag}[\boldsymbol{\mu}(t)]\boldsymbol{\theta}_k) \tag{18}$$

Noting the fact that

$$\begin{aligned}
&\tilde{\boldsymbol{\theta}}_k^{\mathrm{T}}\boldsymbol{\Gamma}_k^{-1}\mathrm{diag}[\boldsymbol{\mu}(\mathrm{t})]\hat{\boldsymbol{\theta}}_k - \boldsymbol{\theta}_k^{\mathrm{T}}\boldsymbol{\Gamma}_k^{-1}\mathrm{diag}[\boldsymbol{\mu}(\mathrm{t})]\boldsymbol{\theta}_k \\
&\quad = \sum_{i=1}^{q}\frac{1}{\kappa_{ki}}\boldsymbol{\mu}_i(t)(\tilde{\boldsymbol{\theta}}_{ki}\hat{\boldsymbol{\theta}}_{ki} - \boldsymbol{\theta}_{ki}^2) \le -\sum_{i=1}^{q}\frac{1}{2\kappa_{ki}}\boldsymbol{\mu}_i(t)(\boldsymbol{\theta}_{ki}^2 + \hat{\boldsymbol{\theta}}_{ki}^2) \le 0
\end{aligned} \tag{19}$$

Finally, the derivative of the candidate Lyapunov function in Eq. (14) satisfies the following inequality:

$$\dot{V}_1 \le -\alpha \boldsymbol{z}_1^{\mathrm{T}}\boldsymbol{z}_1 + \boldsymbol{z}_1^{\mathrm{T}}\hat{\boldsymbol{J}}\boldsymbol{z}_2 - 2\beta\tilde{\boldsymbol{\theta}}_k^{\mathrm{T}}\boldsymbol{Y}_k^{\mathrm{T}}\boldsymbol{s} \tag{20}$$

Remark 1. By calculating we can find that

$$\hat{\boldsymbol{J}}\boldsymbol{z}_2 = \hat{\boldsymbol{J}}\dot{\boldsymbol{q}} - \hat{\boldsymbol{J}}\boldsymbol{\phi} = \hat{\boldsymbol{J}}\dot{\boldsymbol{q}} - \dot{\boldsymbol{x}}_d + \alpha \boldsymbol{z}_1 = \hat{\boldsymbol{s}} \tag{21}$$

This information is helpful in the following controller design procedure.

Step 2: In this step, the purpose is to design the actual control torque to track the given reference joint velocity ϕ. Differentiating Eq. (8) with respect to time t, we can obtain the dynamic equation of $\mathbf{z}_2$

$$\dot{\boldsymbol{z}}_2 = \ddot{\boldsymbol{q}} - \dot{\phi} \tag{22}$$

From (4) we have

$$\begin{aligned}
\boldsymbol{M}(\boldsymbol{q})\dot{\boldsymbol{z}}_2 + \boldsymbol{C}(\boldsymbol{q},\dot{\boldsymbol{q}})\boldsymbol{z}_2 &= \boldsymbol{M}(\boldsymbol{q})\ddot{\boldsymbol{q}} + \boldsymbol{C}(\boldsymbol{q},\dot{\boldsymbol{q}})\dot{\boldsymbol{q}} + \boldsymbol{g}(\boldsymbol{q}) - \boldsymbol{M}(\boldsymbol{q})\dot{\phi} - \boldsymbol{C}(\boldsymbol{q},\dot{\boldsymbol{q}})\phi - \boldsymbol{g}(\boldsymbol{q}) \\
&= \boldsymbol{\tau} + \boldsymbol{\tau}_d - \boldsymbol{Y}_d(\boldsymbol{q},\dot{\boldsymbol{q}},\phi,\dot{\phi})\boldsymbol{\theta}_d
\end{aligned} \tag{23}$$

Multiply $\boldsymbol{z}_2$ to both sides of Eq. (23), it turns to be

$$\boldsymbol{z}_2^{\mathrm{T}}\boldsymbol{M}(\boldsymbol{q})\dot{\boldsymbol{z}}_2 + \boldsymbol{z}_2^{\mathrm{T}}\boldsymbol{C}(\boldsymbol{q},\dot{\boldsymbol{q}})\boldsymbol{z}_2 = \boldsymbol{z}_2^{\mathrm{T}}(\boldsymbol{\tau} + \boldsymbol{\tau}_d - \boldsymbol{Y}_d(\boldsymbol{q},\dot{\boldsymbol{q}},\phi,\dot{\phi})\boldsymbol{\theta}_d) \tag{24}$$

Choosing Lyapunov function as

$$V_2 = V_1 + \tfrac{1}{2}\boldsymbol{z}_2^{\mathrm{T}}\boldsymbol{M}(\boldsymbol{q})\boldsymbol{z}_2 + \tfrac{1}{2}\tilde{\boldsymbol{\theta}}_d^{\mathrm{T}}\boldsymbol{\Gamma}_d{}^{-1}\tilde{\boldsymbol{\theta}}_d + \boldsymbol{\theta}_d^{\mathrm{T}}\mathrm{diag}[\boldsymbol{v}(t)]\boldsymbol{\theta}_d \tag{25}$$

where $\boldsymbol{\Gamma}_d \triangleq \mathrm{diag}[\boldsymbol{\kappa}_{d1},\boldsymbol{\kappa}_{d2},\ldots,\boldsymbol{\kappa}_{dp}]$ is a symmetric positive definite diagonal matrix, and the vector function $\mathbf{v}(t)$ is defined as $\boldsymbol{v}(t) \triangleq [\boldsymbol{v}_1(t),\ \boldsymbol{v}_2(t),\ldots,\ \boldsymbol{v}_p(t)]^{\mathrm{T}}$ with initial values set to be positive. Then the derivative of V_2 along with Eq. (22) is given by

$$\begin{aligned}
\dot{V}_2 &= \dot{V}_1 + \boldsymbol{z}_2^{\mathrm{T}}\boldsymbol{M}(\boldsymbol{q})\dot{\boldsymbol{z}}_2 + \boldsymbol{z}_2^{\mathrm{T}}\boldsymbol{C}(\boldsymbol{q},\dot{\boldsymbol{q}})\boldsymbol{z}_2 - \tilde{\boldsymbol{\theta}}_d^{\mathrm{T}}\boldsymbol{\Gamma}_d^{-1}\dot{\hat{\boldsymbol{\theta}}}_d + \boldsymbol{\theta}_d^{\mathrm{T}}\mathrm{diag}[\dot{\boldsymbol{v}}(t)]\boldsymbol{\theta}_d \\
&\le -\alpha \boldsymbol{z}_1^{\mathrm{T}}\boldsymbol{z}_1 - 2\beta\tilde{\boldsymbol{\theta}}_k^{\mathrm{T}}\boldsymbol{Y}_k^{\mathrm{T}}\boldsymbol{s} + \boldsymbol{z}_2^{\mathrm{T}}(\hat{\boldsymbol{J}}^{\mathrm{T}}\boldsymbol{z}_1 + \boldsymbol{\tau} + \boldsymbol{\tau}_d - \boldsymbol{Y}_d(\boldsymbol{q},\dot{\boldsymbol{q}},\phi,\dot{\phi})\boldsymbol{\theta}_d) \\
&\quad + \boldsymbol{\theta}_d^{\mathrm{T}}\mathrm{diag}[\dot{\boldsymbol{v}}(t)]\boldsymbol{\theta}_d - \tilde{\boldsymbol{\theta}}_d^{\mathrm{T}}\boldsymbol{\Gamma}_d^{-1}\dot{\hat{\boldsymbol{\theta}}}_d
\end{aligned} \tag{26}$$

Designing the adaptive control law as

$$\boldsymbol{\tau} = -\hat{\boldsymbol{J}}^{\mathrm{T}}\boldsymbol{z}_1 - \beta\hat{\boldsymbol{J}}^{\mathrm{T}}\hat{\boldsymbol{s}} - \eta\boldsymbol{z}_2 + \boldsymbol{Y}_d(\boldsymbol{q},\dot{\boldsymbol{q}},\phi,\dot{\phi})\hat{\boldsymbol{\theta}}_d \tag{27}$$

where η is a positive constant.

Let the dynamic parameter estimation error vector be defined as

$$\tilde{\boldsymbol{\theta}}_d \triangleq \boldsymbol{\theta}_d - \hat{\boldsymbol{\theta}}_d \tag{28}$$

Then Eq. (26) can be rewritten in the following form:

$$\begin{aligned}\dot{V}_2 &= -\alpha\boldsymbol{z}_1^{\mathrm{T}}\boldsymbol{z}_1 - \beta\hat{\boldsymbol{s}}^{\mathrm{T}}\hat{\boldsymbol{s}} - \boldsymbol{\eta}\boldsymbol{z}_2^{\mathrm{T}}\boldsymbol{z}_2 - 2\beta\tilde{\boldsymbol{\theta}}_k^{\mathrm{T}}\boldsymbol{Y}_k^{\mathrm{T}}\boldsymbol{s} - \boldsymbol{z}_2^{\mathrm{T}}\boldsymbol{Y}_d(\boldsymbol{q},\dot{\boldsymbol{q}},\phi,\dot{\phi})\tilde{\boldsymbol{\theta}}_d - \tilde{\boldsymbol{\theta}}_d^{\mathrm{T}}\boldsymbol{\Gamma}_d^{-1}\dot{\hat{\boldsymbol{\theta}}}_d \\ &\quad + \boldsymbol{\theta}_d^{\mathrm{T}}\mathrm{diag}[\dot{\boldsymbol{v}}(t)]\boldsymbol{\theta}_d + \boldsymbol{z}_2^{\mathrm{T}}\boldsymbol{\tau}_d \\ &= -\alpha\boldsymbol{z}_1^{\mathrm{T}}\boldsymbol{z}_1 - \beta(\boldsymbol{s} - \boldsymbol{Y}_k\tilde{\boldsymbol{\theta}}_k)^{\mathrm{T}}(\boldsymbol{s} - \boldsymbol{Y}_k\tilde{\boldsymbol{\theta}}_k) - \boldsymbol{\eta}\boldsymbol{z}_2^{\mathrm{T}}\boldsymbol{z}_2 - \tilde{\boldsymbol{\theta}}_d^{\mathrm{T}}(\boldsymbol{Y}_d(\boldsymbol{q},\dot{\boldsymbol{q}},\phi,\dot{\phi})^{\mathrm{T}}\boldsymbol{z}_2 \\ &\quad + \boldsymbol{\Gamma}_d^{-1}\dot{\hat{\boldsymbol{\theta}}}_d) + \boldsymbol{\theta}_d^{\mathrm{T}}\mathrm{diag}[\dot{\boldsymbol{v}}(t)]\boldsymbol{\theta}_d - 2\beta\tilde{\boldsymbol{\theta}}_k^{\mathrm{T}}\boldsymbol{Y}_k^{\mathrm{T}}\boldsymbol{s} + \boldsymbol{z}_2^{\mathrm{T}}\boldsymbol{\tau}_d \\ &= -\alpha\boldsymbol{z}_1^{\mathrm{T}}\boldsymbol{z}_1 - \beta\boldsymbol{s}^{\mathrm{T}}\boldsymbol{s} - \beta(\boldsymbol{Y}_k\tilde{\boldsymbol{\theta}}_k)^{\mathrm{T}}(\boldsymbol{Y}_k\tilde{\boldsymbol{\theta}}_k) + \boldsymbol{z}_2^{\mathrm{T}}\boldsymbol{\tau}_d - \boldsymbol{\eta}\boldsymbol{z}_2^{\mathrm{T}}\boldsymbol{z}_2 \\ &\quad - \tilde{\boldsymbol{\theta}}_d^{\mathrm{T}}(\boldsymbol{Y}_d(\boldsymbol{q},\dot{\boldsymbol{q}},\phi,\dot{\phi})^{\mathrm{T}}\boldsymbol{z}_2\boldsymbol{\Gamma}_d^{-1}\dot{\hat{\boldsymbol{\theta}}}_d) + \boldsymbol{\theta}_d{}^{\mathrm{T}}\mathrm{diag}[\dot{\boldsymbol{v}}(t)]\boldsymbol{\theta}_d\end{aligned} \tag{29}$$

Eq.(29) implies us to choose the following dynamic parameter update law:

$$\dot{\hat{\boldsymbol{\theta}}}_d = -\boldsymbol{\Gamma}_d\boldsymbol{Y}_d(\boldsymbol{q},\dot{\boldsymbol{q}},\phi,\dot{\phi})^{\mathrm{T}}\boldsymbol{z}_2 - \mathrm{diag}[\boldsymbol{v}(t)]\hat{\boldsymbol{\theta}}_d, \dot{\boldsymbol{v}}(t) = -\boldsymbol{\Gamma}_d^{-1}\boldsymbol{v}(t) \tag{30}$$

Subsisting Eq. (30) into Eq. (29) and using the properties given in Section 2 imply that

$$\begin{aligned}&\tilde{\boldsymbol{\theta}}_d^{\mathrm{T}}\boldsymbol{\Gamma}_d^{-1}\mathrm{diag}[\boldsymbol{v}(t)]\hat{\boldsymbol{\theta}}_d - \boldsymbol{\theta}_d^{\mathrm{T}}\boldsymbol{\Gamma}_d^{-1}\mathrm{diag}[\boldsymbol{v}(t)]\boldsymbol{\theta}_d \\ &= \sum_{i=1}^{p}\frac{1}{\boldsymbol{\kappa}_{di}}\boldsymbol{v}_i(t)(\tilde{\boldsymbol{\theta}}_{di}\hat{\boldsymbol{\theta}}_{di} - \boldsymbol{\theta}_{di}^2) \le -\sum_{i=1}^{p}\frac{1}{2\boldsymbol{\kappa}_{di}}\boldsymbol{v}_i(t)(\boldsymbol{\theta}_{di}^2 + \hat{\boldsymbol{\theta}}_{di}^2) \le 0\end{aligned} \tag{31}$$

The derivative of the candidate Lyapunov function turns out to be

$$\dot{V}_2 \le -\alpha\boldsymbol{z}_1^{\mathrm{T}}\boldsymbol{z}_1 - \beta\boldsymbol{s}^{\mathrm{T}}\boldsymbol{s} - \boldsymbol{\eta}\boldsymbol{z}_2^{\mathrm{T}}\boldsymbol{z}_2 - \beta(\boldsymbol{Y}_k\tilde{\boldsymbol{\theta}}_k)^{\mathrm{T}}(\boldsymbol{Y}_k\tilde{\boldsymbol{\theta}}_k) + \boldsymbol{z}_2\boldsymbol{\tau}_d \tag{32}$$

Before giving the conclusions in this paper, we are introducing two lemmas:

Lemma 1. *The following inequalities hold for any vectors* $\mathbf{a},\mathbf{b} \in \mathbb{R}^n$

$$2\boldsymbol{a}^{\mathrm{T}}\boldsymbol{b} \le \boldsymbol{a}^{\mathrm{T}}\boldsymbol{a} + \boldsymbol{b}^{\mathrm{T}}\boldsymbol{b} - 2\boldsymbol{a}^{\mathrm{T}}\boldsymbol{b} \le \boldsymbol{a}^{\mathrm{T}}\boldsymbol{a} + \boldsymbol{b}^{\mathrm{T}}\boldsymbol{b}$$

Lemma 2. (LaSalle–Yoshizawa) (Krstic et al. [13]) *Let* $\boldsymbol{x} = \mathbf{0}$ *be an equilibrium point of system* $\dot{\boldsymbol{x}} = f(\boldsymbol{x},t)$ *and suppose f is locally Lipschitz in* $\boldsymbol{x}$ *uniformly in t. Let* $V : R^n \to R_+$ *be a continuously differentiable, positive definite and radially unbounded function* $V(\boldsymbol{x})$ *such that*

$$\dot{V} = \frac{\partial V}{\partial \boldsymbol{x}}(\boldsymbol{x})\boldsymbol{f}(\boldsymbol{x},t) \le -\boldsymbol{W}(\boldsymbol{x}) \le 0, \quad \forall t \ge 0, \forall \boldsymbol{x} \in R^n \tag{33}$$

where $\boldsymbol{W}$ is a continuous function. Then, all solutions of $\boldsymbol{x} = \boldsymbol{f}(\boldsymbol{x},t)$ are globally uniformly bounded and satisfy

$$\lim_{t\to\infty}\boldsymbol{W}(\boldsymbol{x}(t)) = 0 \tag{34}$$

In addition, if $\boldsymbol{W}(\boldsymbol{x})$ is positive definite, then the equilibrium $\boldsymbol{x} = 0$ is globally uniformly asymptotically stable.

Then we have the following conclusions:

Theorem 1. *Given the robotic system described by Eqs.* (1) and (5), *the control algorithm given by Eqs. (16) and (27) along with the parameter adaptive laws defined in Eqs. (17) and (30). If making the assumption that* $\|\boldsymbol{\tau}_d\| = 0$, *then*

(i) *the asymptotic tracking is achieved, i.e.*

$$\lim_{t\to\infty}(\boldsymbol{x}-\boldsymbol{x}_d)=0 \tag{35}$$

(ii) *the tracking performance is given by*

$$\int_0^\infty (\boldsymbol{x}-\boldsymbol{x}_d)^{\mathrm{T}}(\boldsymbol{x}-\boldsymbol{x}_d)\,\mathrm{d}t \le \frac{1}{\alpha}V_2(0)$$

$$\int_0^\infty (\dot{\boldsymbol{x}}-\dot{\boldsymbol{x}}_d)^{\mathrm{T}}(\dot{\boldsymbol{x}}-\dot{\boldsymbol{x}}_d)\,\mathrm{d}t \le 3\left(\frac{\boldsymbol{\lambda}_{max}\left(\hat{\boldsymbol{J}}^T\hat{\boldsymbol{J}}\right)}{\boldsymbol{\eta}}+\alpha+\frac{1}{\beta}\right)V_2(0) \tag{36}$$

$$V_2(0)=\tfrac{1}{2}\boldsymbol{\theta}_k(0)^{\mathrm{T}}\boldsymbol{\Gamma}_k^{-1}\boldsymbol{\theta}_k(0)+\tfrac{1}{2}\boldsymbol{\theta}_d(0)^{\mathrm{T}}\boldsymbol{\Gamma}_d^{-1}\tilde{\boldsymbol{\theta}}_d(0)+\boldsymbol{\theta}_k^{\mathrm{T}}\mathrm{diag}[\boldsymbol{\mu}(0)]\boldsymbol{\theta}_k+\boldsymbol{\theta}_d^{\mathrm{T}}\mathrm{diag}[v(0)]\boldsymbol{\theta}_d$$

Proof (i). Choosing function V_2 as the candidate Lyapunov function for the robot manipulator system. When $\|\boldsymbol{\tau}_d\| = 0$, from Eq(32) we can obtain

$$\dot{V}_2 \le -\alpha\boldsymbol{z}_1^{\mathrm{T}}\boldsymbol{z}_1-\beta\boldsymbol{s}^{\mathrm{T}}\boldsymbol{s}-\boldsymbol{\eta}\boldsymbol{z}_2^{\mathrm{T}}\boldsymbol{z}_2-\beta(\boldsymbol{Y}_k\tilde{\boldsymbol{\theta}}_k)^{\mathrm{T}}(\boldsymbol{Y}_k\tilde{\boldsymbol{\theta}}_k) \tag{37}$$

From Eq. (37) we established that V_2 is non-increasing. Hence, $\boldsymbol{z}_1,\boldsymbol{z}_2,\hat{\boldsymbol{\theta}}_k,\hat{\boldsymbol{\theta}}_d$are bounded. Because V_2 is a continuously differentiable, positive definite and radially unbounded function. And function $\boldsymbol{W}(\boldsymbol{x}) \triangleq \alpha\boldsymbol{z}_1^{\mathrm{T}}\boldsymbol{z}_1+\beta\boldsymbol{s}^{\mathrm{T}}\boldsymbol{s}+\boldsymbol{\eta}\boldsymbol{z}_2^{\mathrm{T}}\boldsymbol{z}_2+\beta(\boldsymbol{Y}_k\tilde{\boldsymbol{\theta}}_k)^{\mathrm{T}}(\boldsymbol{Y}_k\tilde{\boldsymbol{\theta}}_k)$ is a positive definite function with respect to variables $\boldsymbol{z}_1,\boldsymbol{s},\boldsymbol{z}_2,\boldsymbol{Y}_k\tilde{\boldsymbol{\theta}}_k$. Then by applying Lemma 2, it further follows that $\boldsymbol{z}_1$, $\boldsymbol{s},\boldsymbol{z}_2,\boldsymbol{Y}_k\tilde{\boldsymbol{\theta}}_k$ are globally uniformly asymptotically stable which implies that

$$\lim_{t\to\infty}(\boldsymbol{x}-\boldsymbol{x}_d)=\boldsymbol{0} \tag{38}$$

Proof (ii). From Eq. (37), we also have that

$$\int_0^\infty \boldsymbol{z}_1(\tau)^{\mathrm{T}}\boldsymbol{z}_1(\tau)\,\mathrm{d}\tau \le \frac{1}{\alpha}(V_2(0)-V_2(\infty)) \le \frac{1}{\alpha}V_2(0) \tag{39}$$

Thus, by setting $\boldsymbol{z}_i(0)=0$, $i=1,2$, we obtain

$$\boldsymbol{V}_2(0)=\tfrac{1}{2}\tilde{\boldsymbol{\theta}}_k(0)^{\mathrm{T}}\boldsymbol{\Gamma}_k^{-1}\tilde{\boldsymbol{\theta}}_k(0)+\tfrac{1}{2}\tilde{\boldsymbol{\theta}}_d(0)^{\mathrm{T}}\boldsymbol{\Gamma}_d^{-1}\tilde{\boldsymbol{\theta}}_d(0)+\boldsymbol{\theta}_k^{\mathrm{T}}\mathrm{diag}\left[\boldsymbol{\mu}(0)\right]\boldsymbol{\theta}_k+\boldsymbol{\theta}_d^{\mathrm{T}}\mathrm{diag}[\mathbf{v}(0)]\boldsymbol{\theta}_d \tag{40}$$

which is a decreasing function with respect to each elements of matrix $\boldsymbol{\Gamma}_k,\boldsymbol{\Gamma}_d$, an increasing function with respect to each elements of vectors $\boldsymbol{\mu}(0),\mathbf{v}(0)$. Resulting from Eqs. (39) and (40), this means that the $\mathscr{L}_2$ norm of the tracking error is

$$\int_0^\infty (\boldsymbol{x}-\boldsymbol{x}_d)^{\mathrm{T}}(\mathbf{x}-\boldsymbol{x}_d)\,\mathrm{d}t \le \frac{1}{\alpha}\Big(\frac{1}{2}\tilde{\boldsymbol{\theta}}_k(0)^{\mathrm{T}}\boldsymbol{\Gamma}_k^{-1}\tilde{\boldsymbol{\theta}}_k(0)+\frac{1}{2}\tilde{\boldsymbol{\theta}}_d(0)^{\mathrm{T}}\boldsymbol{\Gamma}_d^{-1}\tilde{\boldsymbol{\theta}}_d(0)$$
$$+\boldsymbol{\theta}_k^{\mathrm{T}}\mathrm{diag}[\boldsymbol{\mu}(0)]\boldsymbol{\theta}_k+\boldsymbol{\theta}_d^{\mathrm{T}}\mathrm{diag}[\mathbf{v}(0)]\boldsymbol{\theta}_d\Big) \tag{41}$$

From Eqs. (7), (8) and (16), we get

$$\int_0^\infty (\dot{\boldsymbol{x}}-\dot{\boldsymbol{x}}_d)^{\mathrm{T}}(\dot{\boldsymbol{x}}-\dot{\boldsymbol{x}}_d)\,\mathrm{d}t=\int_0^\infty (\hat{\boldsymbol{J}}\dot{\boldsymbol{q}}+\boldsymbol{Y}_k\tilde{\boldsymbol{\theta}}_k-\dot{\boldsymbol{x}}_d)^{\mathrm{T}}(\hat{\boldsymbol{J}}\dot{\boldsymbol{q}}+\boldsymbol{Y}_k\tilde{\boldsymbol{\theta}}_k-\dot{\boldsymbol{x}}_d)\,\mathrm{d}t$$

$$
\begin{aligned}
&= \int_0^\infty (\hat{\boldsymbol{J}}\boldsymbol{z}_2 + \hat{\boldsymbol{J}}j + \boldsymbol{Y}_k\tilde{\boldsymbol{\theta}}_k - \dot{\boldsymbol{x}}_d)^{\mathrm{T}}(\hat{\boldsymbol{J}}\boldsymbol{z}_2 + \hat{\boldsymbol{J}}j + \boldsymbol{Y}_k\tilde{\boldsymbol{\theta}}_k - \dot{\boldsymbol{x}}_d)\,\mathrm{d}t \\
&= \int_0^\infty (\hat{\boldsymbol{J}}\boldsymbol{z}_2 - \boldsymbol{\alpha}\boldsymbol{z}_1 + \boldsymbol{Y}_k\tilde{\boldsymbol{\theta}}_k)^{\mathrm{T}}(\hat{\boldsymbol{J}}\boldsymbol{z}_2 - \boldsymbol{\alpha}\boldsymbol{z}_1 + \boldsymbol{Y}_k\tilde{\boldsymbol{\theta}}_k)\,\mathrm{d}t \\
&= \int_0^\infty (\hat{\boldsymbol{J}}\boldsymbol{z}_2)^T(\hat{\boldsymbol{J}}\boldsymbol{z}_2) + \boldsymbol{\alpha}^2\boldsymbol{z}_1{}^{\mathrm{T}}\boldsymbol{z}_1 + (\boldsymbol{Y}_k\tilde{\boldsymbol{\theta}}_k)^{\mathrm{T}}(\boldsymbol{Y}_k\tilde{\boldsymbol{\theta}}_k) - 2(\hat{\boldsymbol{J}}\boldsymbol{z}_2)^{\mathrm{T}}(\alpha\boldsymbol{z}_1) \\
&\quad + 2(\hat{\boldsymbol{J}}\boldsymbol{z}_2)^{\mathrm{T}}(\boldsymbol{Y}_k\tilde{\boldsymbol{\theta}}_k) - 2(\boldsymbol{\alpha}\boldsymbol{z}_1)^{\mathrm{T}}(\boldsymbol{Y}_k\tilde{\boldsymbol{\theta}}_k)\,\mathrm{d}t
\end{aligned} \tag{42}
$$

From Lemma 1 we can further conclude that

$$
\int_0^\infty (\dot{\boldsymbol{x}} - \dot{\boldsymbol{x}}_d)^{\mathrm{T}}(\dot{\boldsymbol{x}} - \dot{\boldsymbol{x}}_d)\,\mathrm{d}t \le 3\int_0^\infty \left((\hat{\boldsymbol{J}}\boldsymbol{z}_2)^{\mathrm{T}}(\hat{\boldsymbol{J}}\boldsymbol{z}_2) + \boldsymbol{\alpha}^2\boldsymbol{z}_1^{\mathrm{T}}\boldsymbol{z}_1 + (\boldsymbol{Y}_k\tilde{\boldsymbol{\theta}}_k)^{\mathrm{T}}(\boldsymbol{Y}_k\tilde{\boldsymbol{\theta}}_k)\right)\mathrm{d}t \tag{43}
$$

Similar to Eq. (39), the following results can be obtained that

$$
\int_0^\infty \boldsymbol{z}_2^{\mathrm{T}}\boldsymbol{z}_2\,\mathrm{d}t \le \frac{\boldsymbol{1}}{\boldsymbol{\eta}} V_2(0) \tag{44}
$$

$$
\int_0^\infty (\boldsymbol{Y}_k\tilde{\boldsymbol{\theta}}_k)^{\mathrm{T}}(\boldsymbol{Y}_k\tilde{\boldsymbol{\theta}}_k) \le \frac{\boldsymbol{1}}{\boldsymbol{\beta}} V_2(0) \tag{45}
$$

Thus, using the property of norm, it can be obtained

$$
\begin{aligned}
\int_0^\infty (\dot{\boldsymbol{x}} - \dot{\boldsymbol{x}}_d)^{\mathrm{T}}(\dot{\boldsymbol{x}} - \dot{\boldsymbol{x}}_d)\,\mathrm{d}t &\le 3\int_0^\infty (\boldsymbol{z}_2\hat{\boldsymbol{J}}^{\mathrm{T}}\hat{\boldsymbol{J}}\boldsymbol{z}_2 + \boldsymbol{\alpha}^2\boldsymbol{z}_1^{\mathrm{T}}\boldsymbol{z}_1 + (\boldsymbol{Y}_k\tilde{\boldsymbol{\theta}}_k)^{\mathrm{T}}(\boldsymbol{Y}_k\tilde{\boldsymbol{\theta}}_k))\,\mathrm{d}t \\
&\le 3\int_0^\infty (\lambda_{max}(\hat{\boldsymbol{J}}^{\mathrm{T}}\hat{\boldsymbol{J}})\boldsymbol{z}_2^{\mathrm{T}}\boldsymbol{z}_2 + \boldsymbol{\alpha}^2\boldsymbol{z}_1^{\mathrm{T}}\boldsymbol{z}_1 + (\boldsymbol{Y}_k\tilde{\boldsymbol{\theta}}_k)^{\mathrm{T}}(\boldsymbol{Y}_k\tilde{\boldsymbol{\theta}}_k))\,\mathrm{d}t \\
&\le 3\left(\frac{\lambda_{max}\left(\hat{\boldsymbol{J}}^{\boldsymbol{T}}\hat{\boldsymbol{J}}\right)}{\boldsymbol{\eta}} + \alpha + \frac{1}{\beta}\right) V_2(0)
\end{aligned} \tag{46}
$$

Thus finish the proof.

Theorem 2. *Given the robotic system described by Eqs.* (1) and (5), *the control algorithm given by Eqs. (16) and (17) along with the parameter adaptive laws defined in Eqs. (17) and (30), when* $\|\boldsymbol{\tau}_d\| \ne 0$, *if the following constraints on the controller parameters holds*

$$
\begin{cases} \alpha \ge \rho_1^2 \\ \beta \ge \rho_2^2 \\ \eta \ge \rho_3^2 + 1/(4\gamma^2) \end{cases} \tag{47}
$$

The close loop system is uniformly bounded sable. And the following disturbance rejection inequality holds:

$$
\|\boldsymbol{y}\|_{\mathscr{L}_2} \le \gamma\|\boldsymbol{\tau}_d\|_{\mathscr{L}_2} + \sqrt{V_2(0)} \tag{48}
$$

Proof. For $\|\boldsymbol{\tau}_d\| \ne 0$, we can define the function H as

$$
H = \dot{V}_2 + \boldsymbol{y}^{\mathrm{T}}\boldsymbol{y} - \gamma^2\boldsymbol{\tau}_d{}^{\mathrm{T}}\boldsymbol{\tau}_d \tag{49}
$$

By calculating we can find that

$$H \leq -\alpha z_1^T z_1 - \beta s^T s - \eta z_2^T z_2 + \rho_1^2 z_1^T z_1 + \rho_2^2 s^T s + \rho_3^2 z_2^T z_2 + z_2^T \tau_d - \gamma^2 \tau_d^T \tau_d$$
$$\leq -(\alpha - \rho_1^2)\|z_1\|^2 - (\beta - \rho_2^2)\|s\|^2 - \left(\eta - \rho_3^2 - \frac{1}{4\gamma^2}\right)\|z_2\|^2 - \left\|\frac{1}{2\gamma} z_2 - \gamma \tau_d\right\|^2 \tag{50}$$

If the parameters α,β,η are chosen to satisfy the inequalities (47), then we can get the following dissipative inequality:

$$\dot{V}_2 \leq \gamma^2 \tau_d^T \tau_d - y^T y \tag{51}$$

Integrating both sides over $[0,\tau]$ yields

$$\int_0^\tau y^T y \, dt \leq \gamma^2 \int_0^\tau \tau_d^T \tau_d \, dt - [V_2(\tau) - V_2(0)] \tag{52}$$

Thus

$$\|y\|_{\mathscr{L}_2} \leq \gamma \|\tau_d\|_{\mathscr{L}_2} + \sqrt{V_2(0)} \tag{53}$$

where we used the facts that $V_2(x) \geq 0$ and $\sqrt{a^2+b^2} \leq a+b$ for nonnegative numbers a and b.

Remark 2. From the proof of Theorem 1, we can find that $Y_k\tilde{\theta}_k$ also converges to zero. In addition, if the persistent excitation conditions is satisfied, the convergence of $\hat{\theta}_k$ to θ_k can be achieved [10]. But this is not true for the dynamic parameters θ_d as we cannot achieve the same results that as time evolves, $Y_d\tilde{\theta}_d$ converges to zero. So we can only get the conclusion that $\hat{\theta}_d$ is bounded which is proved in Theorem 1.

Remark 3. From Theorem 1, the following conclusions can be obtained:

- The tracking performance depends on the initial estimate errors $\tilde{\theta}_k(0),\tilde{\theta}_d(0)$ and the explicit design parameters $\mu(0),\nu(0)$. The smaller the values $\tilde{\theta}_k(0),\tilde{\theta}_d(0)$, $\mu(0),\nu(0)$, the better the transient performance would be.
- The bound for $\int_0^\infty (x-x_d)^T(x-x_d)dt$ is an explicit function of design parameters and thus computable. We can decrease the effects of the initial error on the transient performance by increasing the adaption gain Γ_k,Γ_d.
- To improve the tracking error performance we can also increase the gain α. However, increasing α would influence the performance of $\int_0^\infty (\dot{x}-\dot{x}_d)^T(\dot{x}-\dot{x}_d)dt$. Thus, it is suggested fixing the gain α for some acceptable value and adjust the other gains such as β,η to improve the transient performance.

Remark 4. The selection of controller parameters has direct relations with disturbance suppression performance index γ. The smaller the γ, the better the disturbance suppression effects would be. However, this would result in a greater control torque. So, by appropriately choosing controller parameters, the compromise between control torque and control precision can be obtained.

Remark 5. From the expression of the control law in Eq. (27) we can find that the proposed controller does not need to measure the joint acceleration, thus the robustness and disturbance rejection ability to the controller are enhanced.

Remark 6. The adoption of the functions $\mu(t)$ and $\nu(t)$ increases the stability of the parameter estimation procedure, which to some extent avoids the singularity of the inverse of the Jacobian matrix appearing. In the proposed controller, the kinematic controller's update law containing the inverse of the estimated Jacobian matrix which is assumed to exist when the robot manipulator execute tasks. To reduce the possibility of the singular phenomenon, the project function in Ref. [8] can be used to constrain the range of parameter estimation. But the exact upper and lower bound is needed. Alternatively, the singularity-robust inverse of the approximate Jacobian matrix methods in Ref. [23] can be adopted to bound the virtual input ϕ.

4. Numerical simulation

To study the effectiveness and performance of the proposed formation control strategies, the detailed response is numerically simulated using the set of governing equations of motion Eqs. (1) and (5) in conjunction with the proposed control laws [Eqs. (17) and (31)]. Here, a 2-link planar space robot manipulator is adopted to make a numerical simulation. The configuration of the model is illustrated in Fig. 2.

The physical parameters of this space robot are listed in Table 1, where m_i and I_i are the mass and the moment of inertia of the ith rigid body, respectively, a_i and b_i are shown as Fig. 2

In the simulations, the desired end-effector trajectory of the planar manipulator is chosen to be a circle in inertia space, i.e.

$$\boldsymbol{x}_d = [1.8\cos(t),\ \ 1.8\sin(t)]^{\mathrm{T}} \tag{54}$$

Moreover, to verify the performance of the proposed Adaptive Backstepping Trajectory Tracking Controller (ABTTC), the Approximate Jacobian Adaptive Controller (AJAC) proposed in Ref. [9] is adopted to make a comparison. The controller parameters in Ref. [9] is chosen as $\boldsymbol{K}_v = \mathrm{diag}[2,2]$, $\boldsymbol{K}_p = \mathrm{diag}[10,10]$, $\boldsymbol{K} = \mathrm{diag}[8,8]$, $\boldsymbol{L}_k = \mathrm{diag}[0.2,0.2]$, $\boldsymbol{L}_d = \mathrm{diag}[0.5,0.5]$, $\alpha = 0.01$. In addition, for all numerical examples presented in this section, the position of the center of mass of the spacecraft is set as $\mathbf{r}_{c0} = [0 \quad 0]^{\mathrm{T}}$, the initial configurations are set as $q_0(0) = 0$, $\ q_1(0) = \pi/3$ and $q_2(0) = -2\pi/3$, respectively; the initial velocity is $\dot{q}_0(0) = 0$, $\dot{q}_1(0) = 0$and $\dot{q}_2(0) = 0$, respectively. Accordingly, the initial kinematic

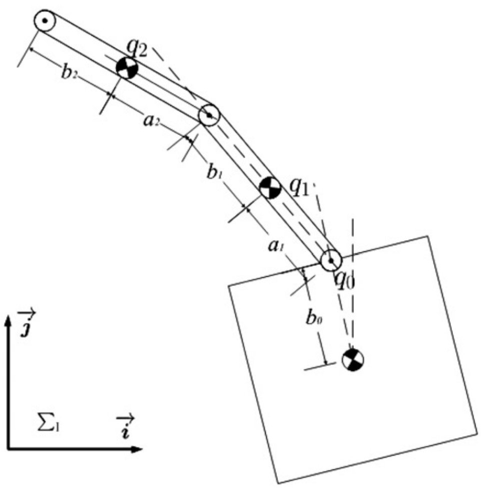

Fig. 2. Configuration of the simulation model.

Table 1
Physical parameters of the space robot manipulator.

Link	a_i (m)	b_i (m)	m_i (kg)	I_i (kg m^2)
Base	–	0.5	40	6.667
1	0.5	0.5	4	0.333
2	0.5	0.5	3	0.250

Table 2
Controller parameters used for numerical analysis.

Control gains	$\mu_i(0)$ $(i=1,2,3)$	$v_i(0)$ $(i=1,\ldots,6)$	$\boldsymbol{\Gamma}_k$	$\boldsymbol{\Gamma}_d$	α	β	η
Value	1	0.01	$2\boldsymbol{I}$	$4\boldsymbol{I}$	1.5	15	100

and dynamic parameter estimates are chosen as

$$\hat{\boldsymbol{\theta}}_k(0) = \begin{bmatrix} 0.8 & 1.3 & 1.5 \end{bmatrix}^{\mathrm{T}}$$
$$\hat{\boldsymbol{\theta}}_d(0) = \begin{bmatrix} 3.0 & 1.0 & 1.0 & 20.0 & 4.0 & 1.0 \end{bmatrix}^{\mathrm{T}} \tag{55}$$

The actual values of the kinematic parameter and dynamic parameter are obtained based on the physical parameter given in Table 1

$$\boldsymbol{\theta}_k = \begin{bmatrix} 0.4225 & 0.8936 & 0.9681 \end{bmatrix}^{\mathrm{T}}$$
$$\boldsymbol{\theta}_d = \begin{bmatrix} 2.1277 & 1.3404 & 0.6383 & 12.9096 & 4.7532 & 0.9521 \end{bmatrix}^{\mathrm{T}} \tag{56}$$

To demonstrate the feasibility of the proposed controller, two different situations are considered in the simulation: (1) without external disturbance, and (2) with the external disturbance. In both cases, the design parameters of the proposed controller are determined are given in Table 2.

4.1. Case 1: disturbance-free

The simulation results are given in the Figs. 3–7. Fig. 3 shows desired and actual paths of the FFSR end-effector when tracking the circle $\boldsymbol{x}_d$. The time responses of the FFSR end-effector tracking errors, control torque, kinematic and dynamic parameter estimates are given in Figs. 4–7, respectively.

When carefully observing the tracking error depicted in Fig. 4(a), we may find that the tracking error converges to zero at the time of 4 s and further after about a time period of 1 s of transient process, the tracking error stays on the zero line permanently. But in Fig. 4(b), it takes almost 30 s for the tracking error to converge to zero and the tracking error oscillates several times before it finally becomes stable. These are also true for the control torque, kinematic and dynamic parameter estimations in Figs. 5–7. All the time response of the control torque, kinematic and dynamic parameter estimation under AJAC method has slower convergence rates and greater oscillation amplitudes when compared with ABTTC method proposed in the paper. Additionally, from Figs. 6 and 7, it can be seen that the estimated kinematic parameters eventually converge to their actual values. However, this is not true for dynamic parameters. But compared with the kinematic parameter estimation procedure, the estimations of dynamic parameters turn into the stable state much quicker than those of the kinematic parameters. The

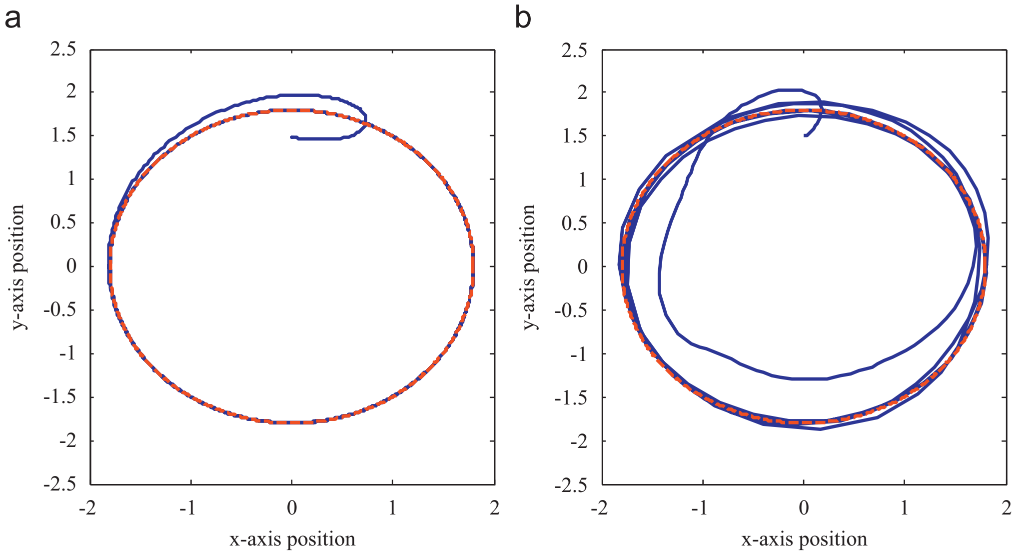

Fig. 3. Path of the end effector: (a) ABTTC method and (b) AJAC method.

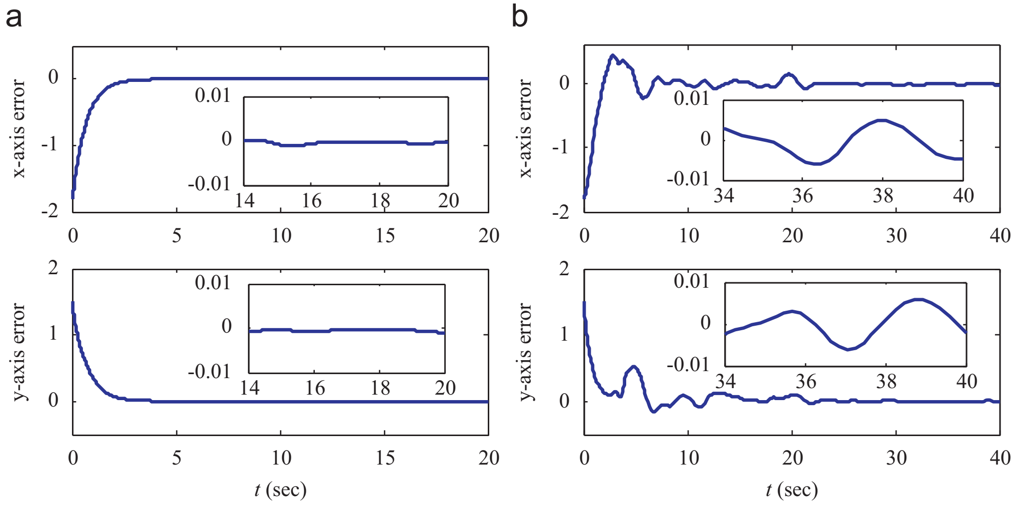

Fig. 4. Time response of end effector tracking error: (a) ABTTC method and (b) AJAC method.

reason may lie in the fact that the kinematic parameter estimation is directly affected by the end effector tracking error.

4.2. Case 2: considering disturbance

In this case, the following disturbance is taken into consideration, i.e.

$$\tau_{d1} = [20 + 5\cos(20t) + 5e^{-3t}, 15 + 5\sin(30t) + 5e^{-2t}, 15 + 5\sin(40t) + 5e^{-t}]^{\mathrm{T}} \tag{57}$$

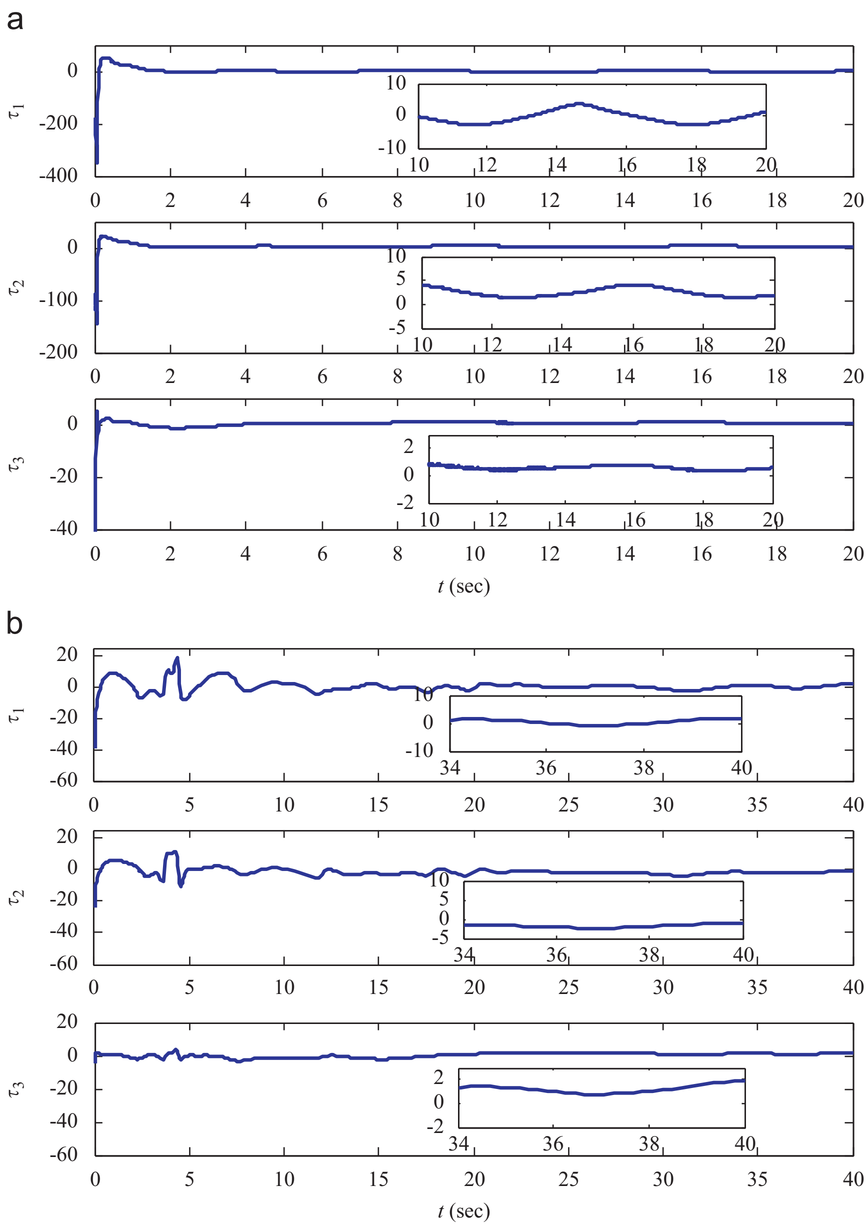

Fig. 5. Time response of control torque: (a) ABTTC method and (b) AJAC method.

If the parameters of the controlled output are chosen as $\rho_1=1,\ \rho_2=1,\ \rho_3=1$, and the L_2 gain is set as $\gamma=0.01$, then we can see that the foregoing controller parameters still satisfy the guidance of Eq. (36). The simulation results are presented in Figs. 8 and 9. From Fig. 9, at first glance, we can find that under sinusoid disturbance the system using ABTTC is still stable, but this is not true for AJAC; actually, in the construction of AJAC in Ref. [9], the author fails to consider the external disturbance. Furthermore, from Fig. 8(a), we

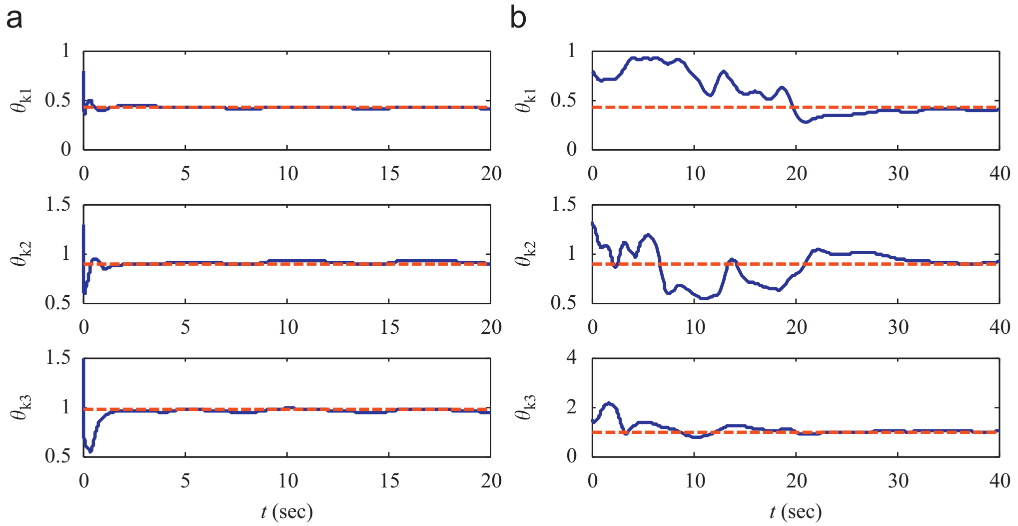

Fig. 6. Time response of kinematic parameter estimation (θ_k-dashed, $\hat{\theta}_k$-solid): (a) ABTTC method and (b) AJAC method.

may find that the tracking performance achieves the same results as the one without disturbance. However, when amplify the tracking error in Fig. 9 to see the details hidden behind and compared with Fig. 4(a), we may find that when there exist no disturbance the tracking converges to zero asymptotically, but when sinusoidal disturbance exists, the tracking error comes out. But the magnitude of the tracking error is as small as 0.005, which to some extent proves the disturbance suppression ability of the proposed controller.

Summarizing all the cases (with and/or without disturbance), it is noted that the proposed controllers design method can significantly improve the system performance without disturbance in both theory and simulations. Also, with disturbance case, the proposed methods have desired results. In addition, extensive simulations were also done using different control parameters, disturbance inputs and even combination of the desired trajectory. These results show that in the closed-loop system the tracking target is accomplished in spite of these undesired effects in the system. Moreover, the flexibility in the choice of control parameters can be utilized to obtain desirable performance while meeting the constraints on the system. These control approaches provides the theoretical basis for the practical application of the advanced control theory to robot manipulator control system.

5. Conclusions

In this paper, we presented a tracking control scheme based on adaptive backstepping for a space robot manipulator system. Kinematic/dynamic uncertainty and external disturbance with an unknown bound were employed in the development of the adaptive parameter update laws. By defining appropriate Lyapunov function, asymptotical stabilization is guaranteed; and also taking the external disturbance into consideration, the dissipative equation is used to ensure the L_2 gain from disturbance to controlled output is less than the required value. In addition, the function of controller parameters is analyzed

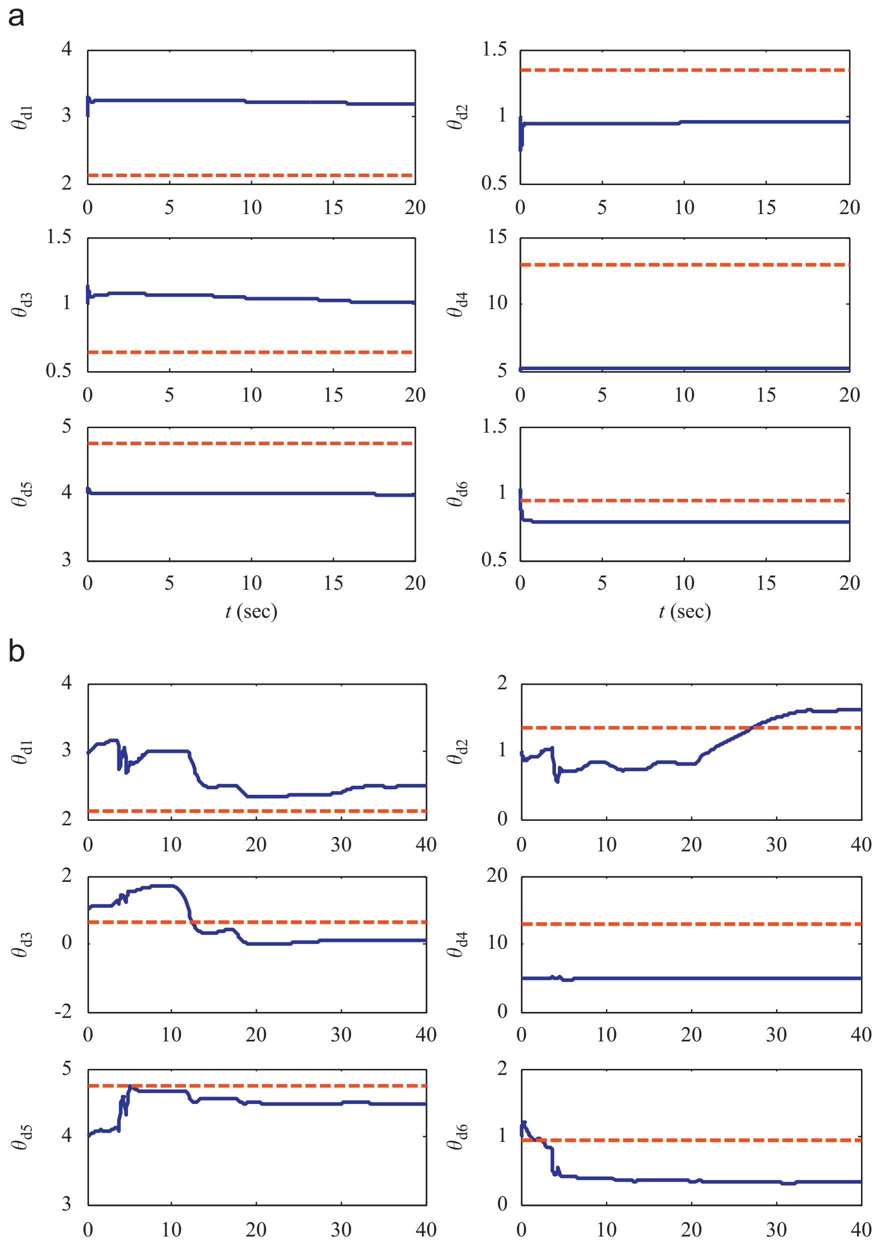

Fig. 7. Time response of dynamic parameter estimation (θ_d-dashed, $\hat{\theta}_d$-solid): (a) ABTTC method and (b) AJAC method.

carefully which provides application instructions and a deeper insight of the controller. The numerical results clearly establish the robustness of the proposed control methodologies in tracking a desired trajectory in the presence of model uncertainties, time-varying disturbances.

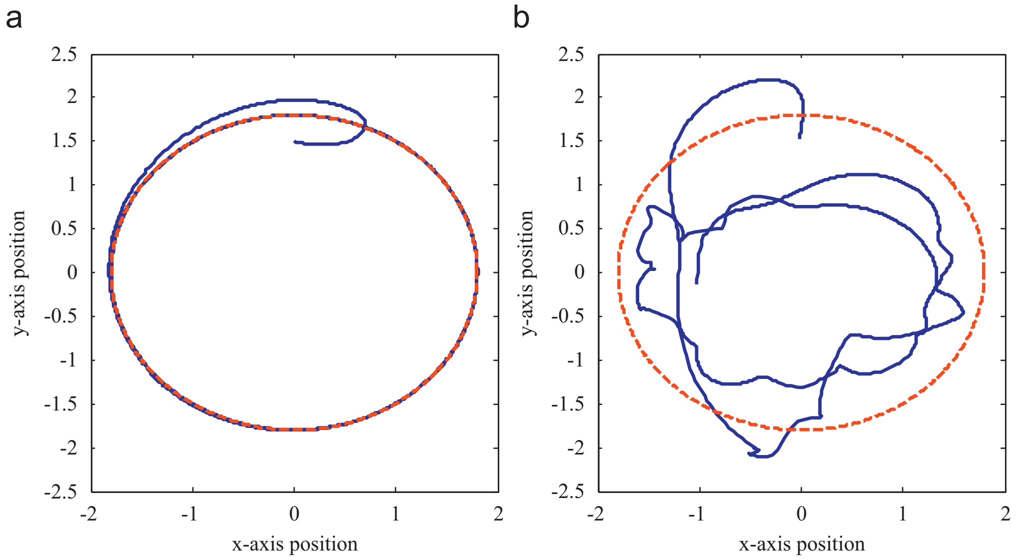

Fig. 8. Path of the end effector: (a) ABTTC method and (B) AJAC method.

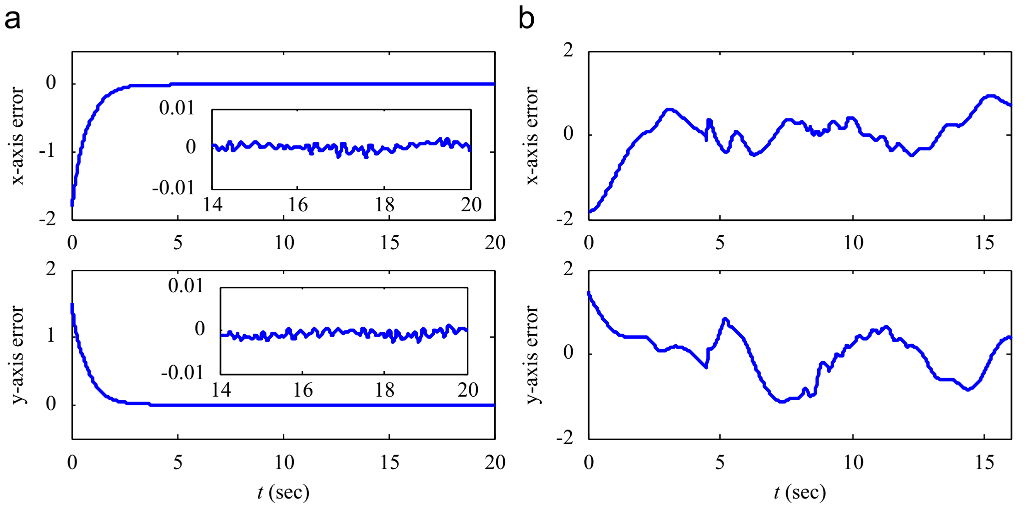

Fig. 9. Time response of end effector tracking error: (a) ABTTC method and (b) AJAC method.

While the simulation results presented in this paper merely illustrate formulations for the particular trajectories tracking, further testing would be required to reach any conclusions about the efficacy of the control and adaptation laws for tracking arbitrary trajectory. In addition, this control scheme places no restriction on the magnitude of the desired control, and the design with explicitly considering the actuator limit is also being investigated. Future work is planned to study the digital implementation of such control scheme on hardware platforms for attitude control experimentation.

Acknowledgments

This present work was supported by the Scientific Research Foundation for National Natural Science Foundation of China (Project nos. 60774062 and 61174200), the Fundamental Research Funds for the Central Universities (Project no. HIT.NSRIF.2009003), Research Fund for Doctoral Program of Higher Education of China (Project no. 20102302110031) and Scientific Research Foundation for the Returned Overseas Chinese Scholars of Harbin (Project no. 2010RFLXG001). The author fully appreciates the financial supports. The author would also like to thank the reviewers and the Editor for many suggestions that helped improve the paper.

References

[1] J. Craig, Ping Hsu, S. Shankar Sastry. Adaptive control of mechanical manipulators, in: IEEE International Conference on Robotics and Automation, Proceedings, 1986, pp. 190–195.
[2] J.J.E. Slotine, W. Li, Adaptive manipulator control: A case study, IEEE Transactions on Automatic Control 33 (11) (1988) 995–1003.
[3] R. Ortega, M.W. Spong, Adaptive motion control of rigid robots: a tutorial, Automatica 25 (6) (1989) 877–888.
[4] H. Berghuis, R. Ortega, H. Nijmeijer., A robust adaptive robot controller, IEEE Transactions on Robotics and Automation 9 (6) (1993) 825–830.
[5] P. Tomei, Robust adaptive friction compensation for tracking control of robot manipulators, IEEE Transactions on Automatic Control 45 (11) (2000) 2164–2169.
[6] C.C. Cheah, S. Kawamura, S. Arimoto, Feedback control for robotic manipulator with uncertain kinematics and dynamics, in: IEEE International Conference on Robotics and Automation, Proceedings, vol. 4, 1998, pp. 3607–3612.
[7] C.C. Cheah, M. Hirano, S. Kawamura, S. Arimoto, Approximate Jacobian control for robots with uncertain kinematics and dynamics, IEEE Transactions on Robotics and Automation 19 (4) (2003) 692–702.
[8] W.E. Dixon, Adaptive regulation of amplitude limited robot manipulators with uncertain kinematics and dynamics, IEEE Transactions on Automatic Control 52 (3) (2007) 488–493.
[9] C.C. Cheah, C. Liu, J.J.E. Slotine. Approximate Jacobian adaptive control for robot manipulators, in: IEEE International Conference on Robotics and Automation, Proceedings, vol. 3, 2004, pp. 3075–3080.
[10] C.C. Cheah, C. Liu, J.J.E. Slotine, Adaptive Jacobian tracking control of robots with uncertainties in kinematic, dynamic and actuator models, IEEE Transactions on Automatic Control 51 (6) (2006) 1024–1029.
[11] C.C. Cheah, C. Liu, J.J.E. Slotine, Adaptive Jacobian tracking control of robots based on visual task-space information, in: IEEE International Conference on Robotics and Automation, Proceedings, 2005 , pp. 3498–3503.
[12] X. Liang, X. Huang, M. Wang, X. Zeng, Adaptive task-space tracking control of robots without task-space- and joint-space-velocity measurements, IEEE Transactions on Robotics 26 (4) (2010) 733–742.
[13] M. Krstic, I. Kanellakopoulos, P.V. Kokotovic., in: Nonlinear and Adaptive Control Design, Wiley, 1995.
[14] Z. Xi, G. Feng, Z.P. Jiang, D. Cheng, Output feedback exponential stabilization of uncertain chained systems, Journal of the Franklin Institute 344 (1) (2005) 36–57.
[15] Z. Jiang, A combined backstepping and small-gain approach to adaptive output feedback control, Automatica 35 (1) (1999) 1131–1139.
[16] I. Ursu, F. Ursu, F. Popescu, Backstepping design for controlling electrohydraulic servos, Journal of the Franklin Institute 343 (1) (2005) 94–110.
[17] K.S. Kim, Y. Kim, Robust backstepping control for slew maneuver using nonlinear tracking function, IEEE Transactions on Control Systems Technology 11 (2003) 822–829.
[18] J. Zhou, Adaptive Backstepping Control of Practical Uncertain Systems, Nanyang Technological University, 2005.
[19] J. Zhou, M. Joo Era, Adaptive output control of a class of uncertain chaotic systems, Systems & Control Letters 56 (6) (2007) 452–460.

[20] J. Zhou, C. Wen, W. Wang, Adaptive backstepping control of uncertain systems with unknown input time-delay, Automatica 45 (6) (2009) 1415–1422.
[21] F. Lewis, C. Abdallah, D. Dawson, Control of Robot Manipulators, MacMillan, New York, 1993.
[22] W.E. Dixon, A. Behal, D.M. Dawson, S. Nagarkatti, Nonlinear Control of Engineering Systems: A Lyapunov-Based Approach, Birkhäuser, Boston, MA, 2003.
[23] Y. Nakamura, in: Advanced Robotics, Addison-Wesley, Reading, MA, 1985.